Supporting Information

Computational Optics Enables Breast Cancer Profiling in Point-of-Care Settings

Jouha Min,[1†] Hyungsoon Im,[1,2†] Matthew Allen,[1] Phillip J. McFarland,[1] Ismail Degani,[1,3] Hojeong Yu,[1] Erica Normandin,[4] Divya Pathania,[1] Jaymin Patel,[5] Cesar M. Castro,[1,6] Ralph Weissleder,[1,2,4*] Hakho Lee[1,2*]

1. Center for Systems Biology, Massachusetts General Hospital, Boston, MA 02114
2. Department of Radiology, Massachusetts General Hospital, Boston, MA 02114
3. Department of Electrical Engineering and Computer Science, Massachusetts Institute of Technology, Cambridge, MA 02139
4. Department of Systems Biology, Harvard Medical School, Boston, MA 02115
5. BreastCare Center, Division of Hematology Oncology, Beth Israel Deaconess Medical Center, Boston, MA, USA
6. Massachusetts General Hospital Cancer Center, Boston, MA 02114

[†] These authors contributed equally to the manuscript

*Corresponding authors: Hakho Lee, PhD, Ralph Weissleder, MD, PhD

hlee@mgh.harvard.edu, rweissleder@mgh.harvard.edu

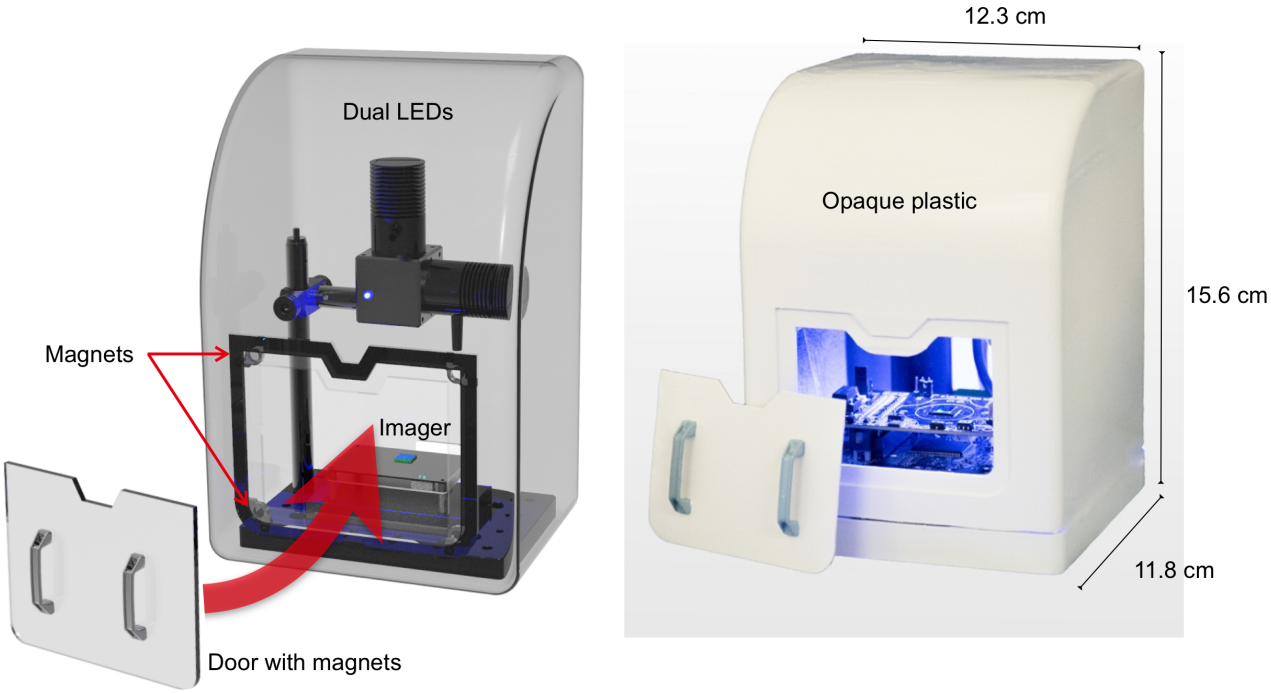

Fig. S1. Stand-alone AIDA device. The imaging component consists of a dual-LED and CMOS image sensor. The device housing was fabricated in a photopolymer resin, and the door was fastened by magnets. The overall size is 11.8 cm (width) × 12.3 cm (length) × 15.6 cm (height).

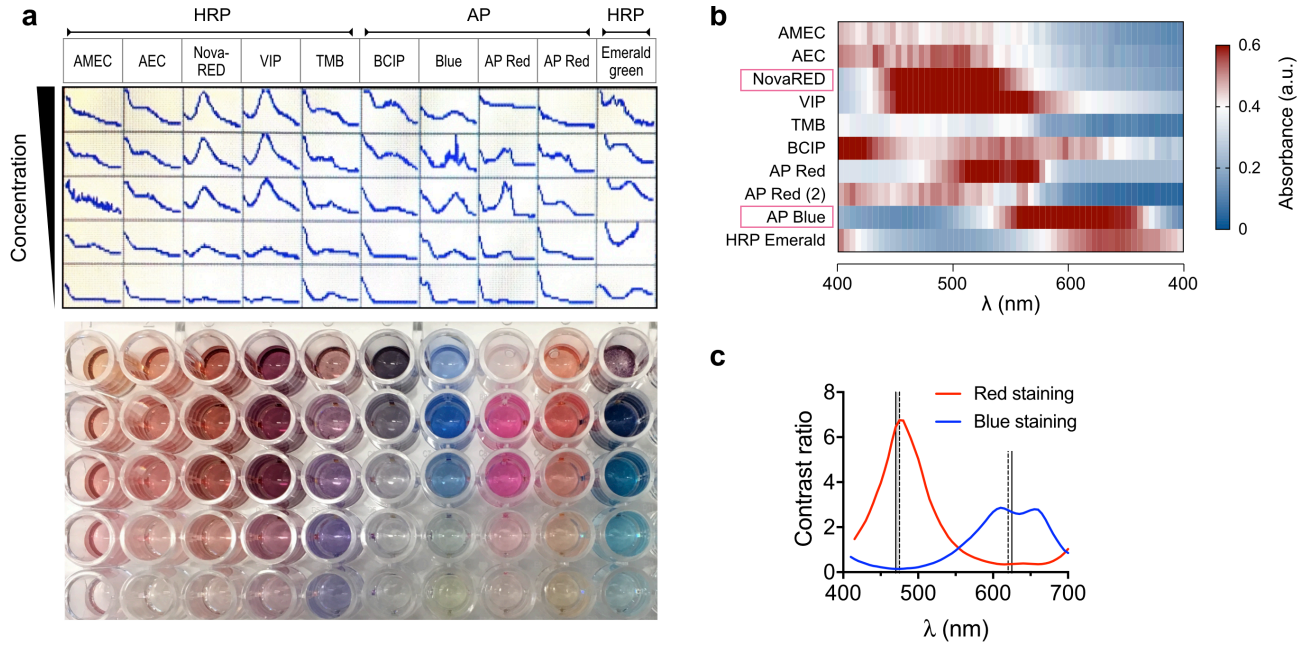

Fig. S2. Chromogenic substrate screening. (a) Absorbance spectra of 10 different chromogenic substrates were measured at different chromogen concentrations. The bottom photo shows the bright-field image of the corresponding dilution series. **(b)** The absorbance levels of the 10 substrates were plotted at a wavelength range of 400 to 700 nm. HRP NovaRED and AP Blue displayed the largest spectral separation and the absorbance difference. **(c)** Choice of illumination wavelength. For red staining, the maximum contrast could be achieved at 475 nm illumination; for blue staining, at 620 nm illumination (dotted lines). LEDs with the closest emission wavelength (solid lines) were chosen.

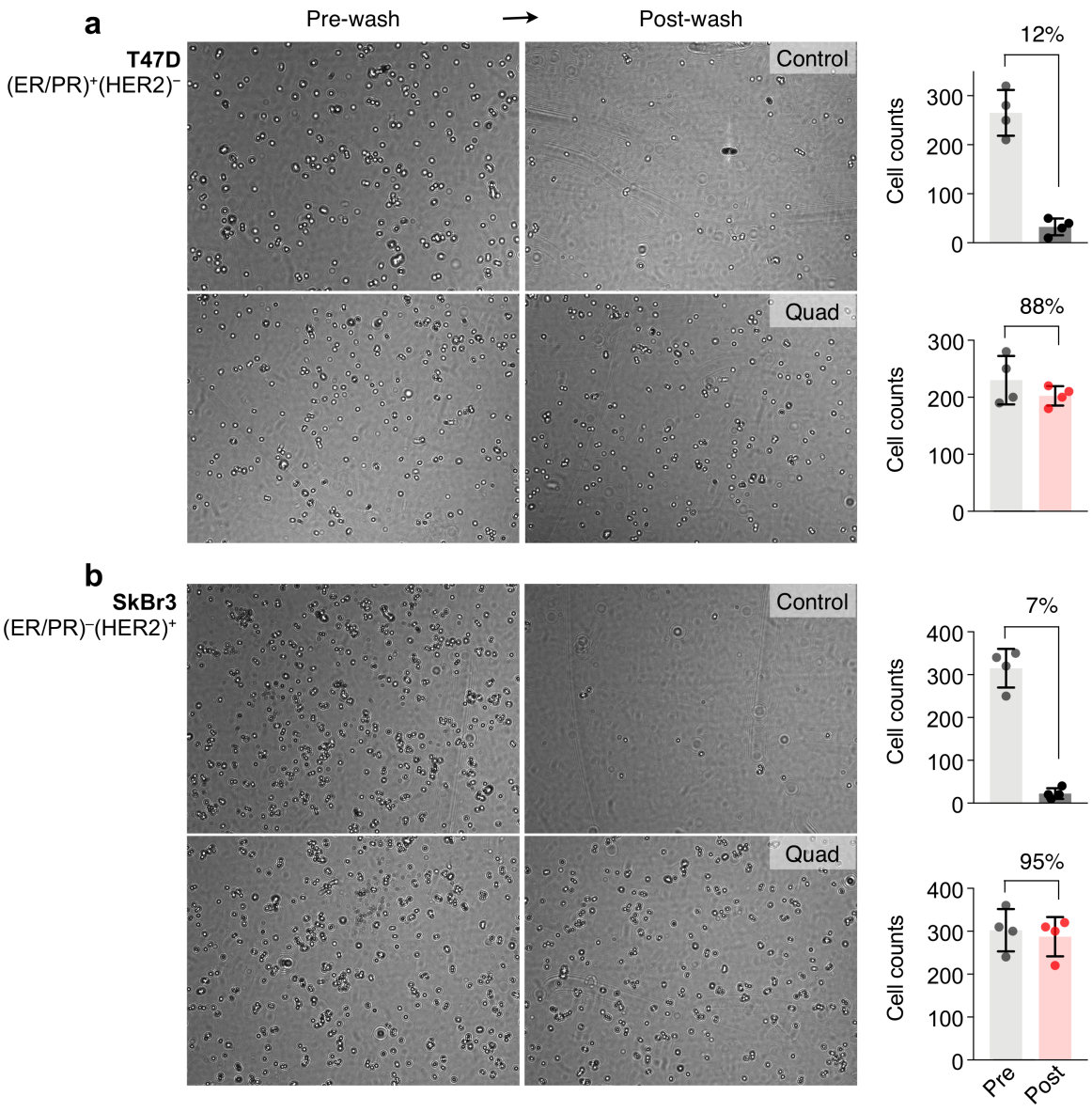

Fig. S3. Cancer cell capture with the quad-marker combination. Different breast cancer cell lines were tested for immunocapture: (a) T-47D and (b) SkBr3. Cells were introduced to a glass substrate coated with a "quad" cocktail of antibodies against HER2, EpCAM, EGFR, and MUC1. The control substrate was coated with isotype-matched IgG antibodies. More than 90% of cancer cells were captured on the quad-marker coated surface, whereas the non-specific binding was <10%. The capture rate for each experiment condition was obtained by analyzing four images. The data are displayed as mean ± SD.

a

	Mounting media	Vendor	Refractive index
1	PBS	Corning	1.33
2	VectaMount AQ Aqueous	Vector Lab	1.44
3	VectaMount Permanent	Vector Lab	1.49
4	Vectashield	Vector Lab	1.45
5	Prolong Diamond	Thermo	1.47
6	Glycerol	Sigma	1.47

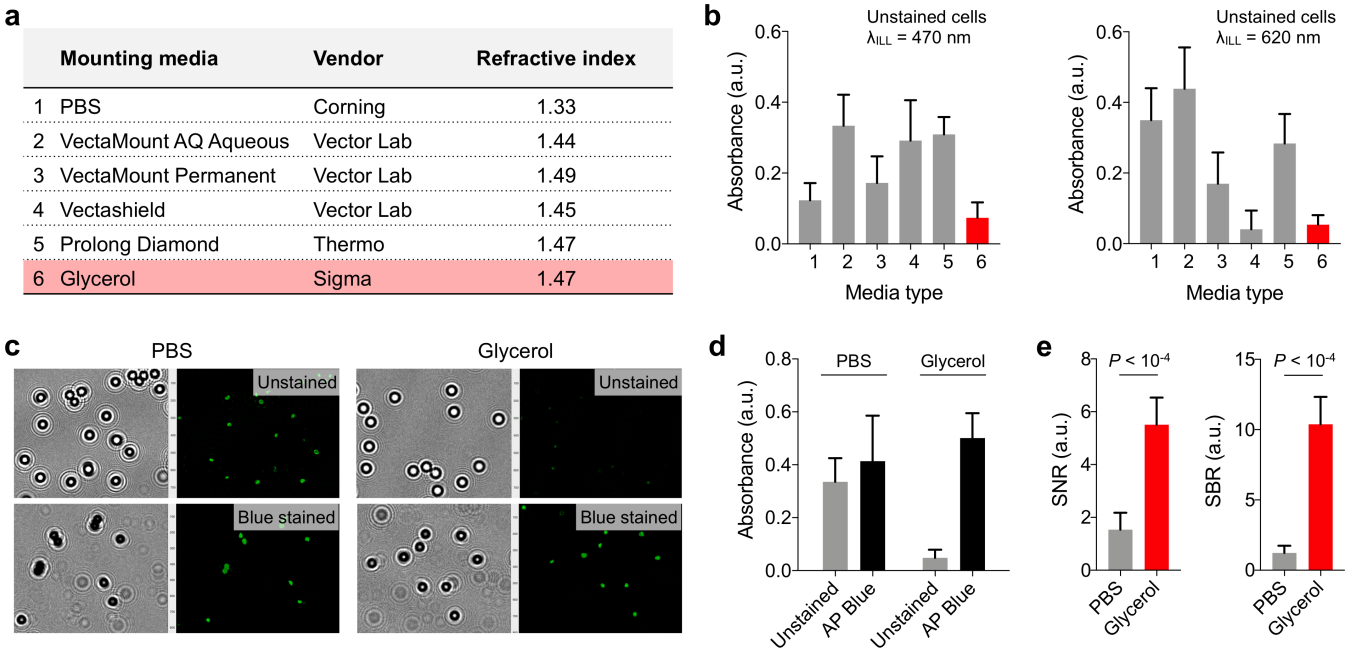

Fig. S4. Index matching strategy. (a) Different types of high refractive index mounting media were tested to reduce optical scattering from unstained cells. **(b)** We embedded cells in the media and imaged them at 470 nm and 625 nm illumination using AIDA. The absorbance of cells was obtained from numerical reconstruction of diffraction patterns. Using glycerol (80%) yielded the lowest absorbance (i.e., optically clear cells) at both illumination wavelengths. Each bar represents mean ± SD from 15 cells. **(c)** Representative images (diffraction and reconstruction) of unstained and stained cells embedded in PBS or 80% glycerol. **(d)** The absorbance of unstained and AP-Blue stained cells (BT4740) were measured in PBS or 80% glycerol media. The index-matching strategy significantly improved the signal contrast. Data are shown as mean ± SD from 33 cells. **(e)** Signal-to-noise ratio (SNR) and signal-to-background ratio (SBR) were compared between PBS and 80% glycerol media solution. Data are shown as mean ± SD from 33 cells.

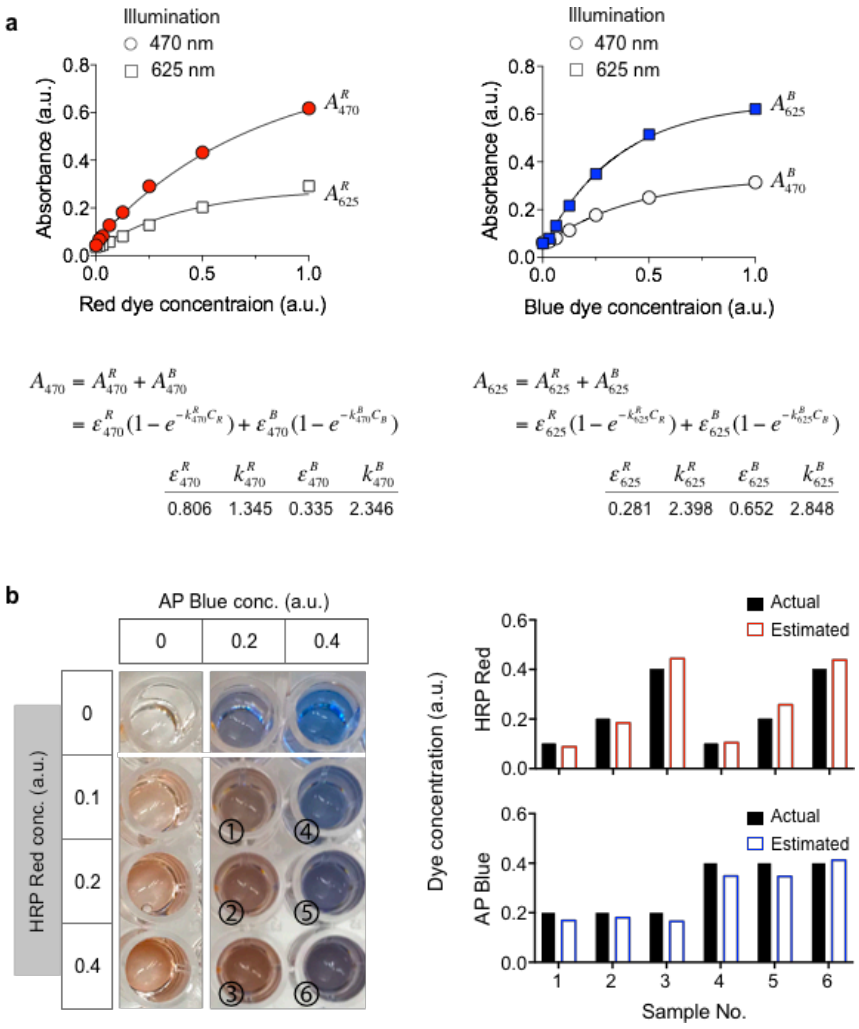

Fig. S5. Converting raw absorbances to dye concentrations. (a) Absorbances of serially diluted dyes (HRP Red, left; AP Blue, right) were measured at two illumination wavelengths (λ_{ILL} = 470 and 625 nm). The curves were fitted to obtain parameters for the total absorbance (A) at each illumination: A_{470} at λ_{ILL} = 470 nm; A_{625} at λ_{ILL} = 625 nm. **(b)** Two dyes (HRP Red and AP Blue) were mixed at different ratios (left), and their total absorbances (A_{470}, A_{625}) were measured. The concentration of each dye type was then estimated from measured absorbances (right).

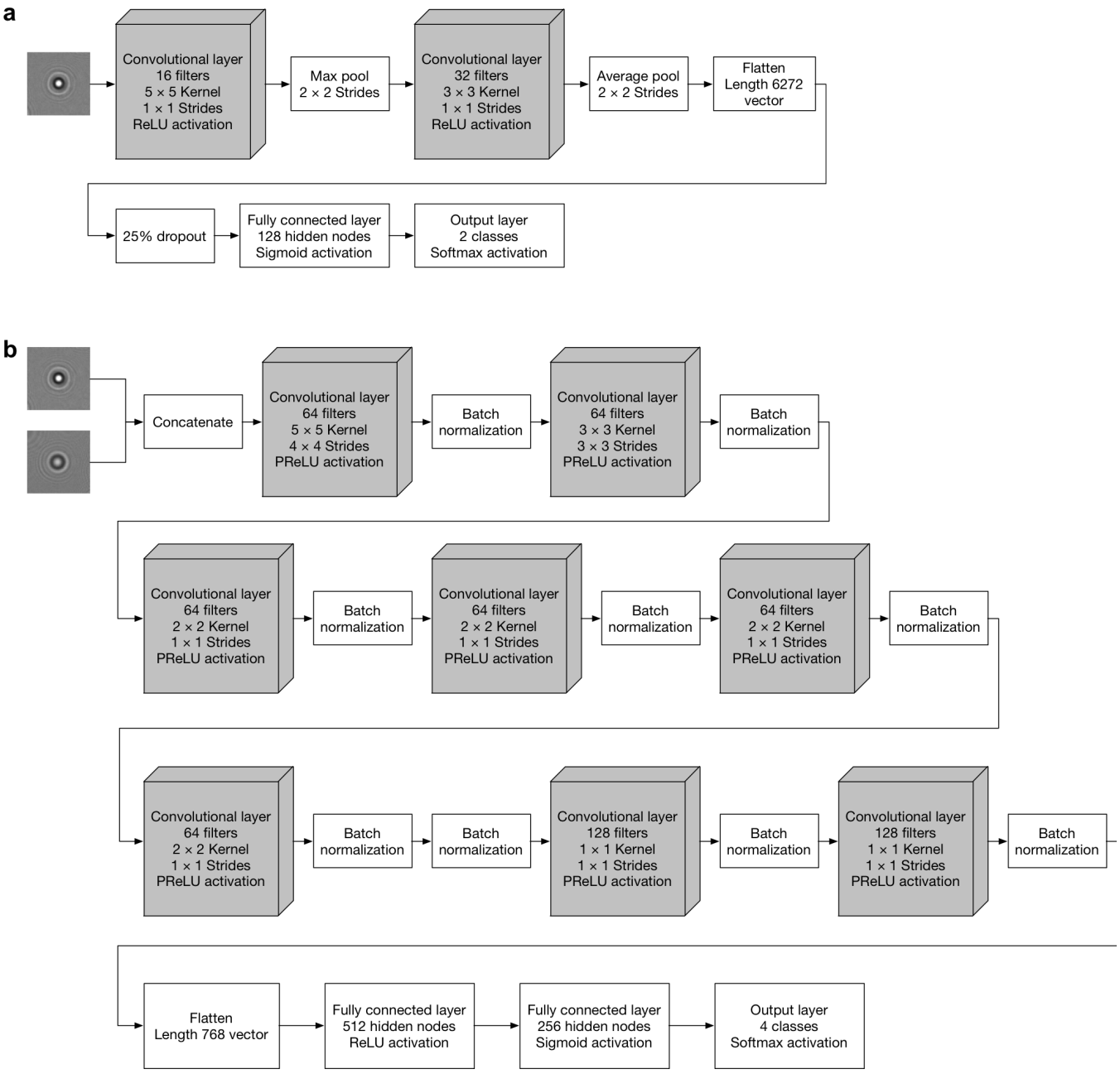

Fig. S6. Architecture of AIDA neural networks. (a) Cell detection network has 2 convolutional layers, 2 pooling layers, and a fully connected layer. The final output has 2 classes (cell, non-cell). **(b)** Color classification network consists of 8 convolutional layers and 3 fully connected layers, and produces the final output of 4 classes (breast cancer subtypes).

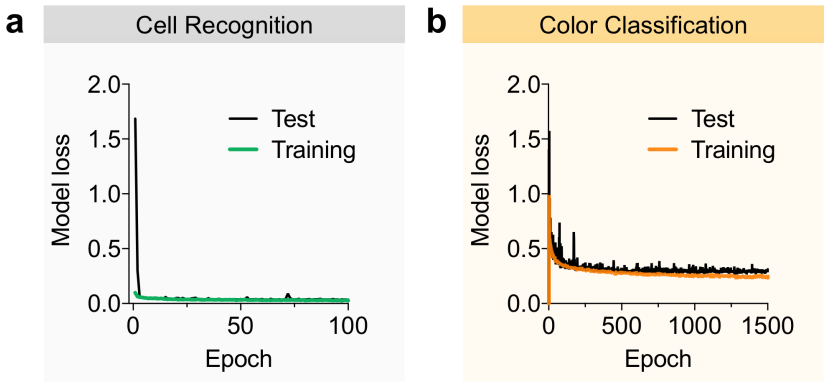

Fig. S7. Model loss for deep neural networks. The loss was estimated using a binary cross-entropy loss function for cell recognition (a) and a categorical cross-entropy loss function for color classification (b).

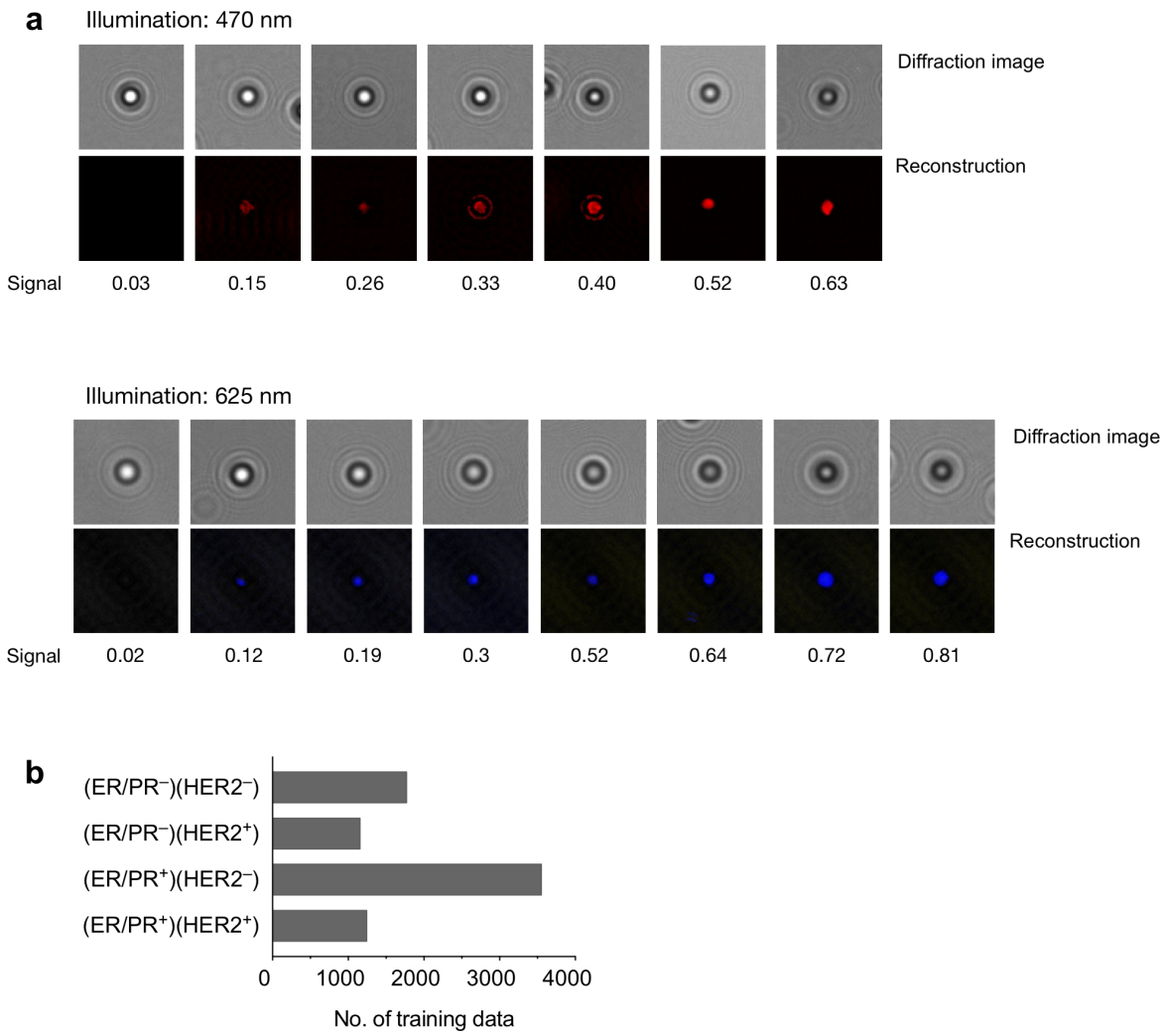

Fig. S8. Training data for deep learning. (a) Over 7,000 diffraction images of cells were taken at 470 nm and 625 nm illumination, and mathematically reconstructed. The diffraction image along with the mean pixel intensity inside each reconstructed cell was used to train the color classification neural network. **(b)** Number of test images used for the color classification training.

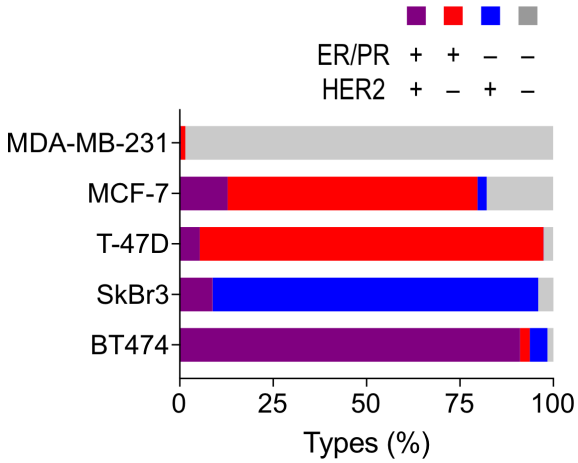

Fig. S9. Flow cytometry-based subtyping. Cancer cell subtyping was done based on ER/PR and HER2 expression. The positive cut-offs for ER/PR and HER2 expression levels were determined according to the conventional criterion: (mean + 2× standard deviation) from the marker expression profiles of negative cell lines.

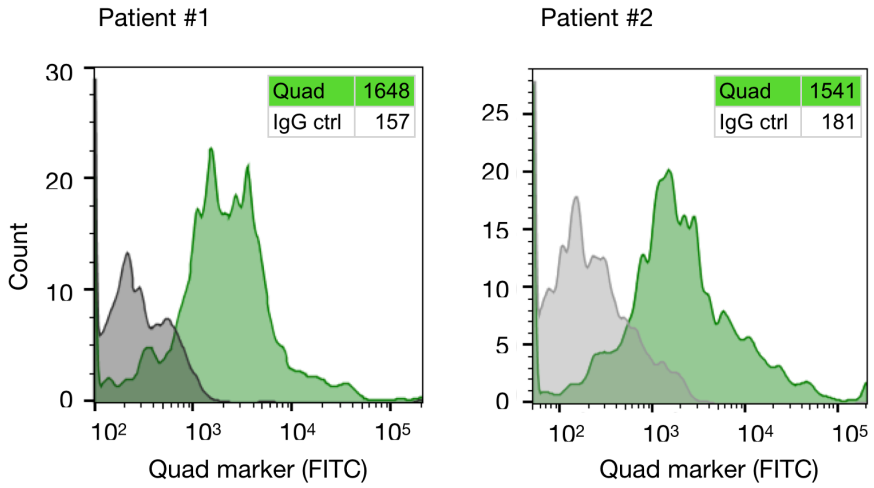

Fig. S10. Representative flow cytometry histograms of patient FNA samples. The samples were treated with the quad-marker (green) or isotype IgG negative control (grey).

Table S1. Cost breakdown for AIDA imaging system and reagent per single assay.

Imaging device components	Cost ($)
Two high power LEDs (470 nm and 625 nm)	100.00
LED driver	60.00
Dichromatic mirror (550 nm cutoff)	75.00
Aperture	20.00
High resolution CMOS image sensor	40.00
Other miscellaneous part components	30.00
3D printed case	20.00
Total	**345.00**

Reagent & Disposable	Price ($)	# of tests	Cost / test ($)
Anti-human ER-a antibody	239.00	100	2.39
Anti-human PR A/B antibody	269.00	200	1.35
Anti-human HER-2 antibody	315.00	1000	0.32
Rabbit IgG, monoclonal isotype control	119.00	1000	0.12
Purified Rat IgG2a, κ Isotype Ctrl Antibody	24.75	1000	0.02
ImmPRESS™ HRP Anti-Rabbit IgG (peroxidase) polymer	140.00	150	0.93
ImmPRESS™ AP Anti-Rat IgG (alkaline phosphatase) polymer	140.00	150	0.93
AP Blue substrate	155.00	500	0.31
ImmPACT NovaRED HRP substrate	144.00	500	0.29
Cell-Tak	205.63	500	0.41
Others (e.g., buffer, tubes)	50.00	100	0.50
Disposable flow cell	2.00	1	2.00
Total			**9.57**

Table S2. List of antibodies used in this study.

Antibody	Clone	Cat No.	Vendor
AIDA			
Anti-human ER-a antibody (rabbit monoclonal)	D6R2W	13258S	CST
Anti-human PR A/B antibody (rabbit monoclonal)	D8Q2J	8757S	CST
Anti-human HER-2 antibody (rabbit monoclonal)	ICR55		BioRad
Rabbit IgG, monoclonal isotype control	DA1E	3900	CST
Purified Rat IgG2a, κ Isotype control antibody		400501	BioLegend
ImmPRESS™ HRP Anti-Rabbit IgG (peroxidase) polymer		MP-7451	Vector Labs
ImmPRESS™ AP Anti-Rat IgG (alkaline phosphatase) polymer		MP-5404	Vector Labs
Flow cytometry			
Anti-human ER-a antibody (rabbit monoclonal)	D6R2W	13258S	CST
Anti-human PR A/B antibody (rabbit monoclonal)	D8Q2J	8757S	CST
Anti-human HER-2 antibody (rat monoclonal)	ICR55		BioRad
Rabbit IgG, monoclonal isotype control	ICR55		BioRad
Purified Rat IgG2a, κ Isotype control antibody	DA1E	3900	CST
Alexa 488 Goat anti-rabbit IgG H&L		4412s	CST
Alexa 647 Goat anti-rabbit IgG H&L		4414s	CST
Alexa 488 Goat anti-rat IgG		405418	BioLegend